Supporting Information

Fabrication of Reversible Poly(dimethylsiloxane) Surfaces via Host-Guest Chemistry and Their Repeated Utilization in Cardiac Biomarker Analysis

Yanrong Zhang,[†,‡] Li Ren,[†,‡] Qin Tu,[†,‡] Xueqin Wang,[‡] Rui Liu,[‡] Li Li,[‡] Jian-Chun Wang,[‡] Wenming Liu,[‡] Juan Xu[‡] and Jinyi Wang[‡,§]*

[‡] Colleges of Science and Veterinary Medicine, Northwest A&F University, Yangling, Shaanxi 712100, P. R. China.

[§] Shaanxi Key Laboratory of Molecular Biology for Agriculture, Northwest A&F University, Yangling, Shaanxi 712100, P. R. China.

Abstract

The Supporting Information includes all additional information as noted in the manuscript and detailed discussions on the current study.

Synthesis of 3-(2-bromoisobutyramido)propyl(trimethoxy) silane (BrTMOS). Scheme S1 shows the synthesis of 3-(2-bromoisobutyramido)propyl(trimethoxy) silane (BrTMOS). Briefly, an anhydrous tetrahydrofuran (THF) solution (15 mL) of 3-aminopropyltrimethoxysilane (1.75 mL, 10 mmol) and

triethylamine (TEA, 1.68 mL, 12 mmol) was cooled to 0 °C. 2-Bromoisobutyryl bromide (1.5 mL, 12 mmol) was then added dropwise to the solution. The mixture was stirred at room temperature for 3 h under a nitrogen atmosphere. Triethylammonium bromide was then removed via filtration and the filtrate was condensed to ~5 mL. The residue from the second precipitation of the bromide salt was removed via centrifugation, and the residual solution was dried at 70 °C for 3 h. ^{1}H NMR (300 MHz, CDCl$_3$): δ 6.90 (s, 1H), 3.58 (s, 9H), 3.30–3.20 (m, 2H), 1.95 (s, 6H), 1.70–1.60 (m, 2H), 0.67 (t, 2H, J = 8.1 Hz), which was the same as previously reported data.[1]
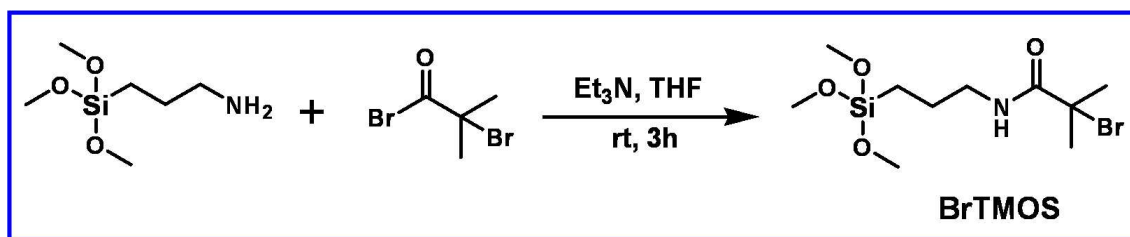

Scheme S1. Synthesis of the SI-ATRP initiator BrTMOS.

Synthesis of Alkynyl and PEG-modified β-CD. To facilitate the conjugation of β-CD onto the PDMS surface and improve its protein-repelling properties, β-CDs were modified using alkynyl groups and PEG units, which was performed using a four-step reaction. The detailed synthetic procedures (Scheme S2) are as follows:

Under a nitrogen atmosphere, a solution of tetraethylene glycol (1 g, 5.15 mmol) in THF (10 mL) was added dropwise to a THF solution of NaH (0.31 g, 60% suspension in oil, 7.8 mmol, 1.5 equiv.) at 0 °C. The reaction mixture was gradually warmed to room temperature for 2 h, and propargyl bromide (0.61 g, 5.15 mmol, 1.0 equiv.) was subsequently added dropwise. The resulting mixture was stirred at room temperature for 6 h and then cooled to 0 °C. Cooled saturated NH$_4$Cl was slowly added to the reaction mixture, which was extracted with ethyl acetate three times. The organic phase was washed with saturated NaCl and dried over anhydrous Na$_2$SO$_4$. The crude product (Compound **S1** in Scheme S2) was purified through silica gel column chromatography (eluent: petroleum ether/ethyl acetate, 1:1). Yield: 57%. MS (ESI): [M+Na]$^+$ calcd for C$_{11}$H$_{20}$O$_5$Na 255.13, found 255.10; ^{1}H NMR (400 MHz, CDCl$_3$): δ 4.16 (d, 2H, J = 2.4 Hz), 3.70–3.50 (m, 16H), 2.89 (br, 1H), 2.41 (t, 1H, J = 2.4 Hz). The MS and ^{1}H

NMR data are the same as those reported previously.[2]
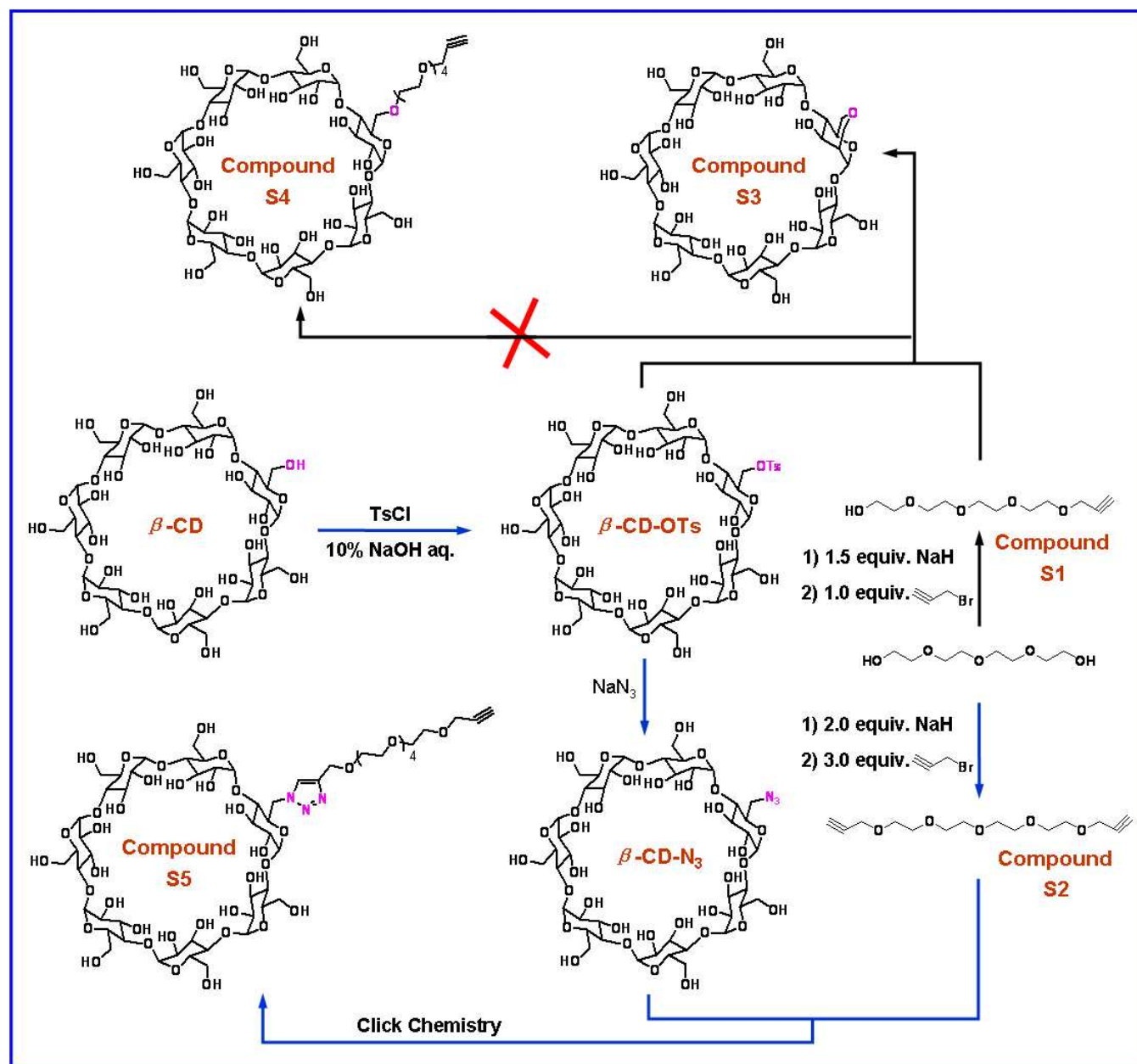
Scheme S2. Synthesis of alkynyl- and PEG-modified β-cyclodextrin (β-CD). To obtain alkynyl- and PEG-modified β-CD, two synthetic protocols were designed in the present study. In the first protocol (top part), the reaction between Compound **S1** and **β-CD-OTs** produced Compound **S3**, and not **S4**. In the second protocol (bottom part), the reaction between Compound **S2** and **β-CD-N$_3$** via click chemistry successfully yielded the expected alkynyl- and PEG-modified β-CD, Compound **S5**.

The synthetic procedure for dual alkynyl-modified tetraethylene glycol (Compound **S2** in Scheme S2) was the same as that for Compound **S1,** except that the ratio of NaH to tetraethylene glycol and the ratio

of propargyl bromide to tetraethylene glycol were 3:1 and 2:1, respectively. Yield: 74%. MS (ESI): [M+Na]$^+$ calcd for $C_{14}H_{22}O_5Na$ 293.15, found 293.19; ^1H NMR (300 MHz, CDCl$_3$): δ 4.21 (d, 4H, J = 2.4 Hz), 3.70–3.60 (m, 16H), 2.45 (t, 2H, J = 2.4 Hz). The MS and ^1H NMR data are the same as those reported previously.[3]

To obtain the target alkynyl and PEG-modified β-CD, two synthetic protocols were designed after the synthesis of Compounds **S1** and **S2** in the current study (top and bottom parts in Scheme S2, respectively).

In the first protocol (top part in Scheme S2), a nucleophilic substitution of the hydroxyl groups of Coumpound **S1** was attempted using the monosubstituted β-CD derivative (**β-CD-OTs** in Scheme S2) to synthesize the target Compound **S4** in a basic medium. Briefly, **β-CD-OTs** was prepared through a conventional procedure using tosylation.[4] Compound **S1** (0.46 g, 1.98 mmol) in N,N-dimethylformamide (DMF, 5 mL) was added dropwise to an anhydrous DMF (10 mL) with NaH (39.6 mg, 1.65 mmol) at 0 °C under a nitrogen atmosphere. The resulting reaction mixture was gradually warmed to room temperature and stirred at this temperature for 0.5 h. Afterward, **β-CD-OTs** (328 mg, 1.98 mmol) was added to the reaction mixture in one portion. The reaction mixture was gradually heated to 80 °C and stirred at this temperature overnight. DMF was removed under vacuum, and the residue was obtained via precipitation with acetone [water:acetone = 1:8 (v/v)]. In this protocol, the 3,6-anhydro-β-CD derivative Compound **S3**, and not **S4**, was obtained.[5] The structure of Compound **S3** was confirmed via matrix-assisted laser desorption ionization time-of-flight mass spectroscopy (MALDI-TOF MS) and ^1H NMR. MALDI-TOF MS: [M+Na]$^+$ calcd for $C_{42}H_{68}O_{34}Na$ 1139.3, found 1139.2; ^1H NMR (500 MHz, D$_2$O): δ 4.99 (s, 7H), 3.90–3.75 (m, 28H), 3.60–3.50 (m, 14H). The MS and ^1H NMR data are the same as those previously reported.[6]

The second synthetic option (bottom part in Scheme S2), click chemistry, was used to obtain the target alkynyl- and PEG-modified β-CD (Compound **S5** in Scheme S2). **β-CD-OTs** were reacted with NaN$_3$ to obtain mono-6-deoxy-6-azido-β-cyclodextrin (**β-CD-N$_3$** in Scheme S2).[7] Afterward, Compound **S2** (0.95 g, 3.5 mmol), **β-CD-N$_3$** (1.16 g, 1 mmol), N,N,N',N'',N''-pentamethyldiethylenetriamine (210

µL, 1 mmol), and dried DMF (20 mL) were added to a Schlenk tube equipped with a magnetic stirring bar. The resultant mixture was degassed via three freeze-thaw cycles, and CuBr (143 mg, 1 mmol) was added under a nitrogen atmosphere. After stirring the mixture at room temperature for 24 h, DMF was removed under vacuum, and the product was precipitated using acetone [water:acetone = 1:8 (v/v)]. The obtained solid was dialyzed against water using a Molecular/Por ultrafiltration flat membrane (500 Da molecular weight cut-off; Molecular/Por®, Spectrum Laboratories, Inc.), and lyophilized for 24 h (VirTis Bench Top 2K freeze dryer, USA). Yield: 59%. The success of the click reaction in producing Compound **S5** was confirmed by the appearance of a single peak at 8.02 ppm in the ^{1}H NMR spectrum,[8] which corresponds to the methane proton in the triazole ring, and the MALDI-TOF MS data. MALDI-TOF MS: [M+Na]$^+$ calcd for $C_{56}H_{91}N_3O_{39}Na$ 1452.5, found 1452.3.

XPS Analysis. The success of each PDMS modification step was confirmed through XPS analysis. A number of wafer-molded PDMS substrates with dimensions of 1.0 cm×1.0 cm were treated for subsequent surface XPS characterizations according to the same approach used to obtain the PDMS-Br, PDMS-PEG-Br, PDMS-PEG-N$_3$, and PDMS-PEG-CD substrates. Figure S1(A) shows the low-resolution XPS survey spectra of each PDMS modification step. The survey spectrum of native PDMS shows three elements: oxygen, carbon, and silicon. Compared with native PDMS, the presence of Br3d and N1s peaks in the survey spectrum of surface PDMS-Br at 68.6 and 398.2 eV, respectively, implies that the SI-ATRP initiator BrTMOS was grafted onto the PDMS-OH surfaces. Further evidence of the existence of the PDMS-Br surface was supported by its high-resolution XPS spectra [Figures S1(B) and S1(C) and Table S1].[9] The high-resolution C1s XPS spectra of the PDMS-Br surface show peaks at 283.2 eV (*C*–H/*C*–Si), 284.6 eV (*C*–Br/*C*–NHCO), and 286.4 eV (O=*C*–N). Comparison with the high-resolution C1s XPS spectra of the native PDMS [282.5 eV (*C*–Si/*C*–H)] indicates that BrTMOS was successfully covalently immobilized on the PDMS surface.
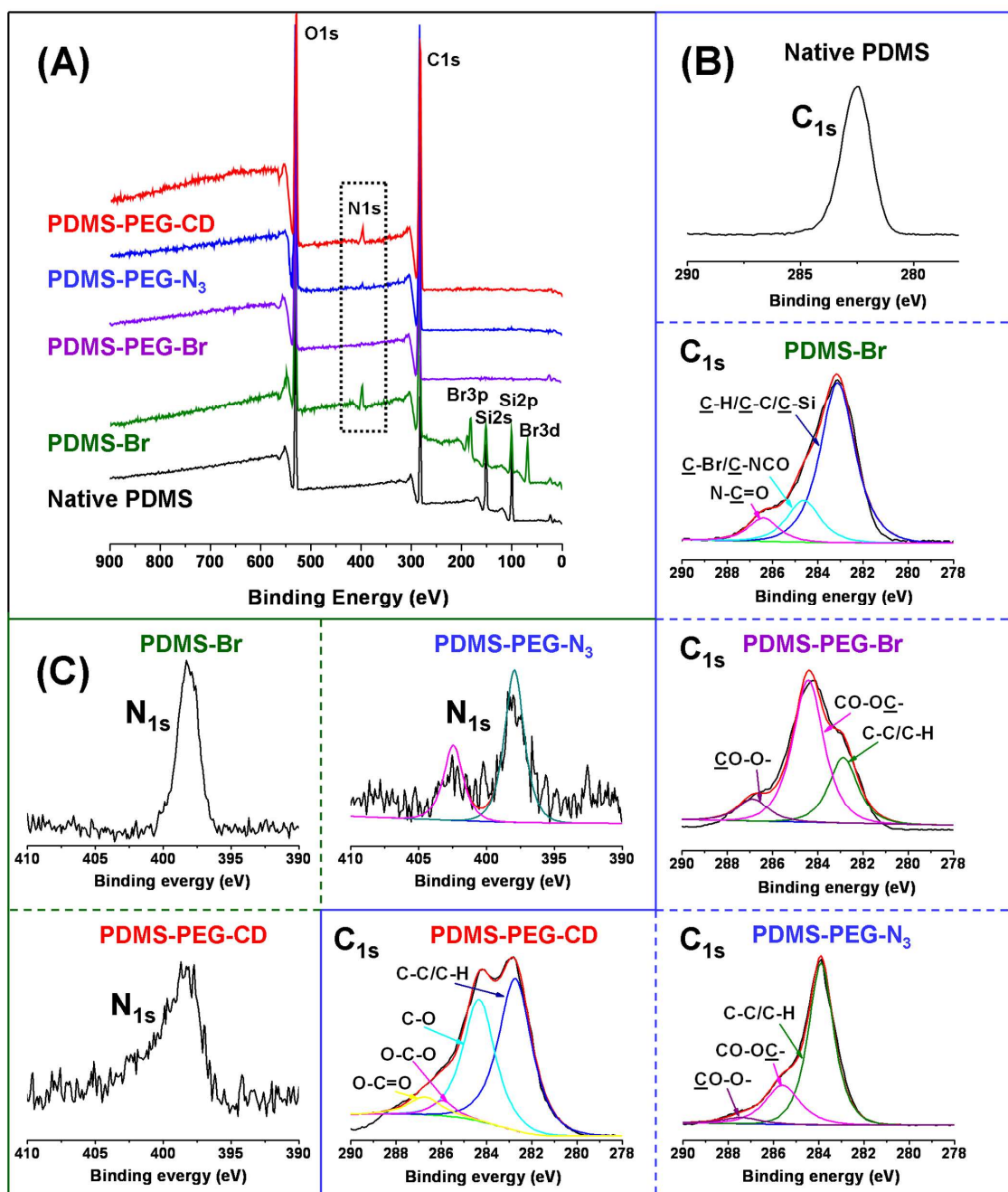
Figure S1. (A) XPS wide-scan spectra of native PDMS, BrTMOS-grafted PDMS (PDMS-Br), PEG-grafted PDMS (PDMS-PEG-Br), azide-grafted PDMS (PDMS-PEG-N$_3$), and alkynyl and PEG-modified β-CD-grafted PDMS (PDMS-PEG-CD); (B) high-resolution XPS C1s spectra of native PDMS, PDMS-Br, PDMS-PEG-Br, PDMS-PEG-N$_3$, and PDMS-PEG-CD; (C) high-resolution XPS N1s spectra of PDMS-Br, PDMS-PEG-N$_3$, and PDMS-PEG-CD.

The chemical composition of the PDMS-PEG-Br surface shown in the low-resolution XPS survey

spectra [Figure S1(A)], which indicate the presence of carbon and oxygen and the absence of nitrogen, bromine, and silicon, strongly support the efficient grafting of the polymer brush to the PDMS surface. The survey spectra also indicate that the thickness of the grafted polymer brush layer was greater than the escape depth of the photoelectrons (~10 nm).[10] Further evidence of the PDMS-PEG-Br surface is given by its high-resolution XPS spectra [Figure S1(B) and Table S1]. A detailed analysis of the C1s signal shows the presence of three different types of carbon atoms (indicated by the peaks at 286.9, 284.4, and 282.9 eV), which can be assigned to the ester groups (O–C=O), ethylene glycol units (C–O), and aliphatic backbone atoms (C–C/C–H) of the polymer brush, respectively.[1] These results indicate that the PEG polymer brush was grafted onto the PDMS-Br surface.

Table S1. Elemental composition of each step of the modification process

Substrate	Elemental Composition (%)					Ratio
	O1s	N1s	C1s	Si2p	Br3d	O/C
Native PDMS	28.63	……	49.17	22.20	……	0.58
PDMS-Br	21.56	4.02	59.59	11.71	3.12	0.36
PDMS-PEG-Br	27.23	……	72.75	……	0.02	0.37
PDMS-PEG-N$_3$	24.39	0.79	74.82	……	……	0.33
PDMS-PEG-CD	28.35	2.51	69.14	……	……	0.41

In the survey XPS spectrum of surface PDMS-PEG-N$_3$ [Figure S1(A)], the appearance of the N1s peak implies the introduction of azide groups. The high-resolution N1s XPS spectra [Figure S1(C)] of the PDMS-PEG-N$_3$ surface show two peaks at 397.95 and 402.45 eV, with a 2:1 peak area ratio. The low- and high-binding energy peaks are respectively assigned to the two nearly equivalent azide N atoms and to the central electron-deficient N atom in the azide group.[11] These findings demonstrate that the azide groups were covalently grafted onto the PDMS-PEG-Br surfaces.

The XPS survey spectrum [Figure S1(A)] of the PDMS-PEG-CD surface indicates the presence of carbon, oxygen, and nitrogen. The peak at 402.45 eV is absent in the high-resolution N1s XPS spectra of the PDMS-PEG-CD surface and that at 397.95 eV is broadened [Figure S1(C)] compared with the

surface PDMS-PEG-N$_3$ spectrum, indicating the complete transformation of the azide group into the 1,2,3-triazole unit.[11] A more detailed analysis was performed through the deconvolution of the high-resolution C1s signals [Figure S1(B)]. Compared with those of PDMS-PEG-N$_3$, the new peak at 285.9 eV (O–C–O) indicates that β-CD was covalently conjugated to the PDMS surfaces.[12] The foregoing results demonstrate that the alkynyl and PEG-modified β-CDs were successfully grafted onto the PDMS surfaces through click chemistry between the alkynyl and azido groups. This finding was also confirmed by the ATR-FTIR spectra (Figure S2), in which the intensity of the asymetric N$_3$ stretching peak at 2031 cm^{-1} disappeared and the new characteristic peak around 1647 cm^{-1} appeared due to the triazole ring formation.[13]

Attenuated Total Reflection Fourier Transform Infrared (ATR-FTIR) Spectroscopic Analysis.

The FT-IR spectra of the modified PDMS substrates were obtained using an EQUINOX-55 FTIR spectrophotometer in the range of 4000–500 cm^{-1}. The modified surfaces were analyzed using the internal ATR mode, in which the PDMS substrates (10 cm×1 cm) were pressed against a Ge hemisphere crystal with minimal pressure to assure optical contact. A single ATR from the interface of the Ge hemisphere crystal and the PDMS substrates was obtained from 16 scans at 4 cm^{-1} resolution. The critical incident angle $\theta_c = 45°$ was used in the current work. The results are shown in Figure S2.
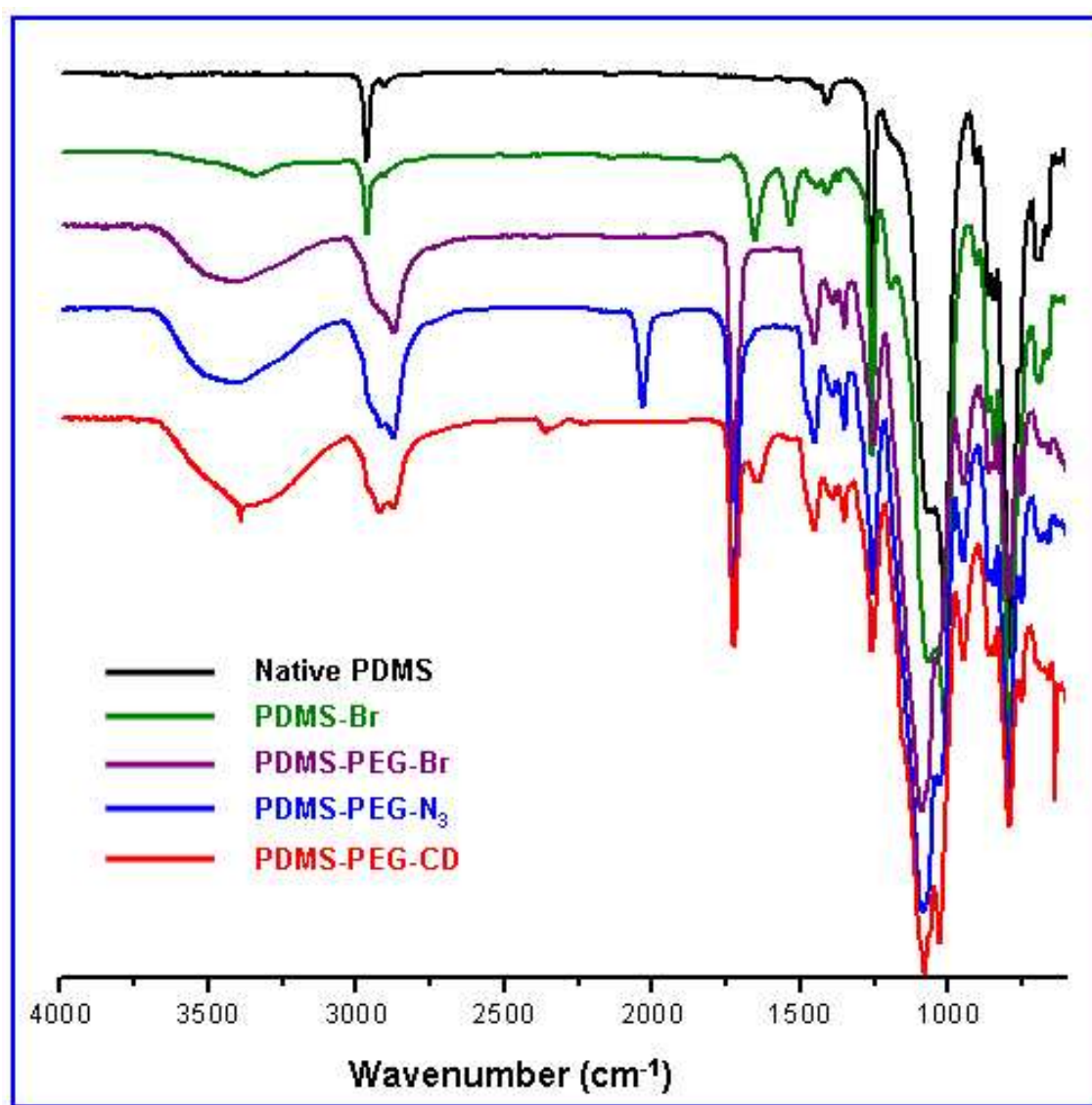

Figure S2. ATR-FT-IR analysis of the native PDMS surface (black line), PDMS-Br surface (olive line), PDMS-PEG-Br surface (violet line), PDMS-PEG-N$_3$ surface (blue line), and PDMS-PEG-CD surface (red line).
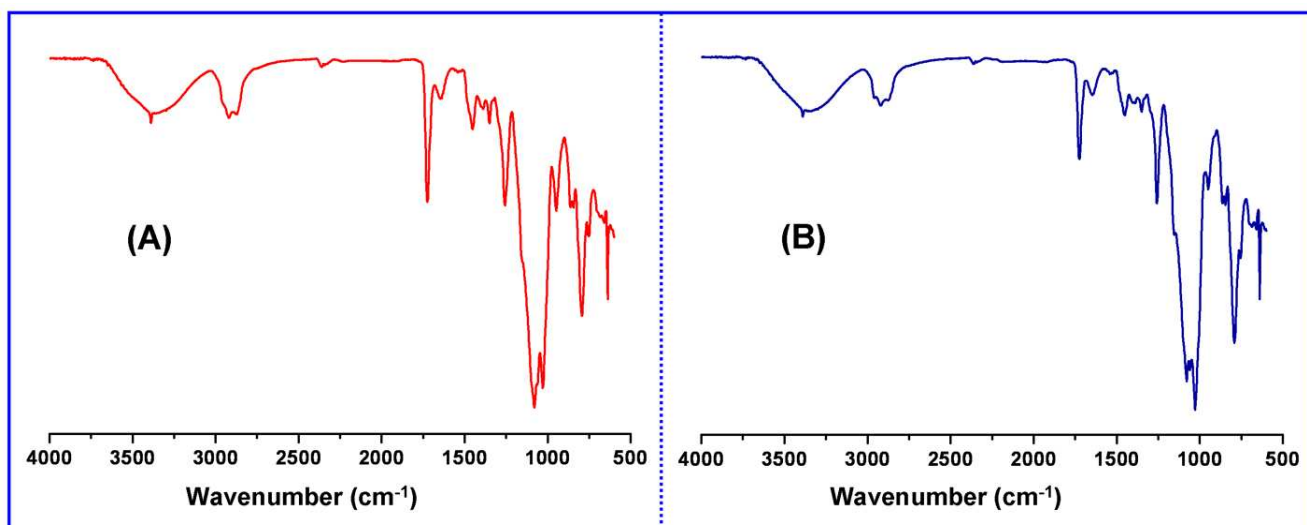
Figure S3. A comparative analysis of the ATR-FT-IR spectra of the prepared PDMS-PEG-CD surface (A) and the PDMS-PEG-CD surface stored under ambient conditions for 30 days (B).

Synthesis of Amino-terminated and PEG-modified Azobenzene (Compound S9 in Scheme S3). Amino-terminated and PEG-modified azobenzene (Compound **S9** in Scheme S3) was synthesized using a four-step reaction (Scheme S3) to facilitate the conjugation of fluorophores and antibodies in azobenzene.
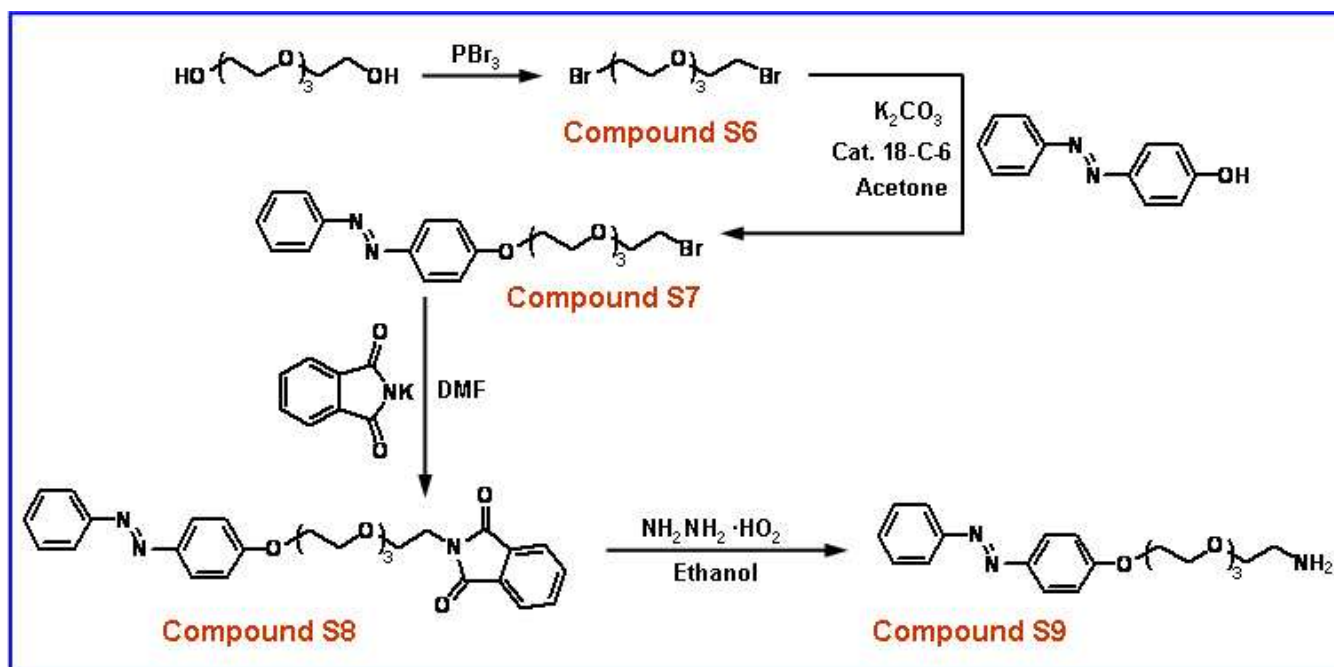
Scheme S3. Synthesis of amino-terminated and PEG-modified azobenzene (Compound **S9**).

Compound 6: Under a nitrogen atmosphere, PBr_3 (2.5 mL, 0.026 mol) was added dropwise to tetraethylene glycol at 0 °C. The reaction mixture was then heated to 60 °C, and stirred at this temperature overnight. Water (20 mL) was slowly added to the mixture at 0 °C to terminate the reaction. After extraction with $CHCl_3$ three times, the organic phase was sequentially washed with an aqueous solution of NaCl, $NaHCO_3$, and again with NaCl, then dried over anhydrous Na_2SO_4. The resulting solution was purified through a silica gel column to obtain Compound **S6**. Yield: 82%. MS (ESI): $[M+Na]^+$ calcd for $C_8H_{16}Br_2O_3Na$, 342.94, found 342.97; ^1H NMR (300 MHz, $CDCl_3$): δ 3.82 (t, 4H, J = 6.3 Hz), 3.69 (s, 8H), 3.49 (t, 4H, J = 6.3 Hz). The MS and ^1H NMR data are the same as those previously reported.[14]

Compound S7: Compound **S6** (2.58 g, 7.0 mmol, 5.0 equiv.) was added to an anhydrous acetone solution (60 mL) of *p*-phenylazophenol (0.28 g, 1.4 mmol, 1.0 equiv.). Anhydrous K_2CO_3 (0.77 g, 5.6 mmol, 4.0 equiv.) and a catalytic amount of 18-C-6 was then added to the resultant yellow solution, and the reaction mixture was refluxed for 24 h under a nitrogen atmosphere. The product (Compound **S7**) was purified via silica gel column chromatography (eluent: petroleum ether/ethyl acetate, 5:1). Yield: 56%. MS (ESI): $[M+Na]^+$ calcd for $C_{20}H_{25}BrN_2O_4Na$, 459.10, found 459.27; ^1H NMR (300 MHz, $CDCl_3$): δ 7.93–7.89 (m, 4H), 7.52–7.41 (m, 3H), 7.03 (d, 2H, J = 9.0 Hz), 4.13 (t, 2H, J = 4.8 Hz), 3.82 (t, 2H, J = 4.8 Hz), 3.76–3.45 (m, 10H), 3.43 (t, 2H, J = 6.3 Hz); ^{13}C NMR (125 MHz, $CDCl_3$): 161.34, 152.70, 147.01, 130.47, 129.09, 124.78, 122.64, 114. 87, 71.16, 70.84, 70.67, 70.60, 70.49, 69.58, 67.74, 30.57; IR (v, cm^{-1}): 2872.2, 1599.4, 1500.3, 1250.7, 1138.6, 839.8, 768.1, 689.7.

Compound S8: Compound **S7** (1.57 g, 3.59 mmol) and phthalimide potassium salt (1.3 g, 7.18 mmol) were dissolved in 25 mL of DMF under a nitrogen atmosphere. After stirring the reaction mixture at 80 °C overnight, the solvent was removed under vacuum, and the residue was purified through silica gel column chromatography (eluent: petroleum ether/ethyl acetate, 1:1). Yield: 89%. MS (ESI): $[M+Na]^+$ calcd for $C_{28}H_{29}N_3O_6Na$, 526.21, found 526.27; ^1H NMR (500 MHz, $CDCl_3$): δ 7.86 (d, 4H, J = 9.0 Hz), 7.84 (d, 2H, J = 7.0 Hz), 7.61–7.59 (m, 2H), 7.45 (t, 2H, J = 7.5 Hz), 7.39 (d, 1H, J = 7.5 Hz), 6.97 (d,

2H, J = 9.0 Hz), 4.13 (t, 2H, J = 5.0 Hz), 3.84 (t, 2H, J = 6.0 Hz), 3.80 (t, 2H, J = 5.0 Hz), 3.70 (t, 2H, J = 6.0 Hz), 3.65–3.55 (m, 8H); ^{13}C NMR (125 MHz, CDCl$_3$): δ 168.14, 161.29, 152.66, 146.95, 133.89, 132.05, 130.39, 129.03, 124.71, 123.14, 122.56, 114.82, 70.78, 70.63, 70.56, 70.09, 69.53, 67.88, 67.69, 37.24; IR: (v, cm^{-1}) 2889.6, 1712.1, 1602.6, 1500.9, 12494, 1105.1, 845.9, 769.6, 720.2, 684.5.

Compound S9: Compound **S8** (1.5 g, 3 mmol) was dissolved in ethanol (25 mL) and hydrazine hydrate (0.75 mL, 80% aqueous) was added to the reaction mixture, which was subsequently stirred overnight at 80 °C. After the removal of the solvent, the residue was purified through silica gel column chromatography (eluent: dichloromethane/methanol/TEA, 75:25:1). Yield: 83%. MS (ESI): [M+H]$^+$ calcd for C$_{20}$H$_{28}$N$_3$O$_4$, 374.20, found 374.19; ^{1}H NMR (500 MHz, CDCl$_3$, ppm): δ 7.92–7.85 (m, 4H), 7.52–7.40 (m, 3H), 7.03 (d, 2H, J = 11.8 Hz), 4.21 (t, 2H, J = 6.0 Hz), 3.89 (t, 2H, J = 6.0 Hz), 3.80–3.61 (m, 8H), 3.51 (t, 2H, J = 6.3 Hz), 2.87 (t, 2H, J = 6.3 Hz), 2.16 (s, 2H); ^{13}C NMR (125 MHz, CDCl$_3$, ppm): δ 161.15, 152.71, 147.04, 130.40, 129.03, 124.73, 122.57, 114.86, 70.82, 70.78, 70.58, 70.52, 69.55, 67.72, 52.10, 41.19; IR (v, cm^{-1}): 3368, 2871.9, 1597.8, 1499.5, 1249.8, 1103.2, 840.6, 768.3, 688.4.

Synthesis of Rhodamine B-labeled Azobenzene (Compound S12 in Scheme S4). Scheme S4 shows the process of the synthesis of rhodamine B-labeled azobenzene (Compound **S12**).
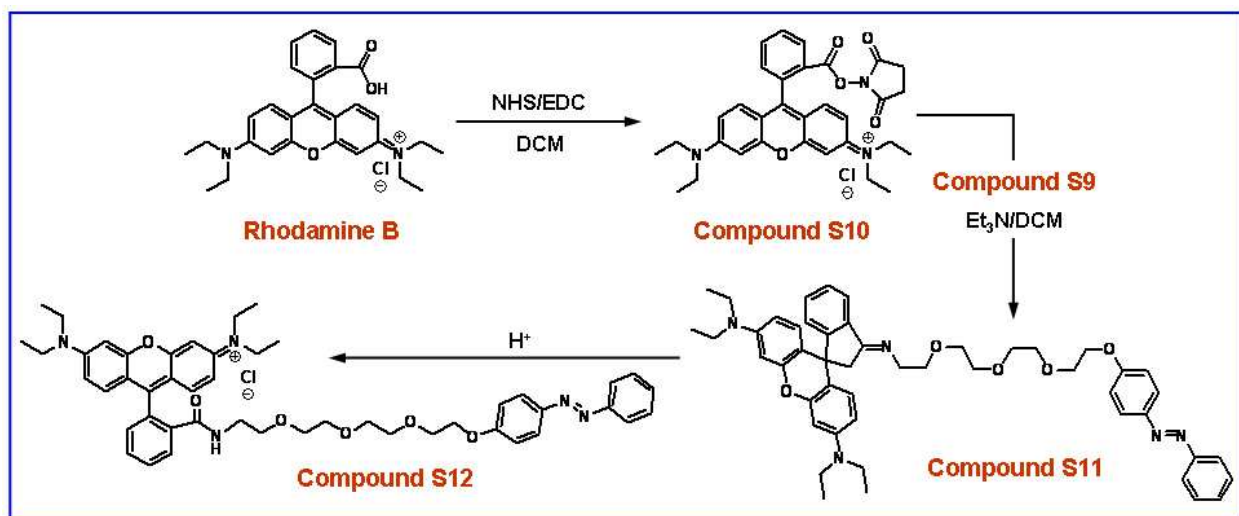
Scheme S4. Synthesis of rhodamine B-labeled azobenzene (Compound **S12**).

Compound S10: N-hydroxysuccinimide (0.264 g, 2.3 mmol) and 1-ethyl-3-(3'-dimethylaminopropyl) carbodiimide (1.21 g, 3.14 mmol) were added to a solution of rhodamine B (1 g, 2.09 mmol) in dried dichloromethane (DCM, 50 mL). The reaction mixture was stirred under a nitrogen atmosphere at room temperature for 12 h. The product was purified via chromatography (methanol:DCM = 1:15). Yield: 79%. MS (ESI): [M–Cl]$^+$ calcd for $C_{32}H_{34}N_3O_5$, 540.25, found 540.21. ^{1}H NMR (500 MHz, CDCl$_3$): δ 8.44 (d, 1H, J = 8.0 Hz), 8.00 (t, 1H, J = 7.0 Hz), 7.85 (t, 1H, J = 7.8 Hz), 7.51 (d, 1H, J = 7.5 Hz), 7.11 (s, 1H), 7.09 (s, 1H), 6.90 (s, 4H), 3.67 (q, 8H, J = 7.0 Hz), 2.79 (s, 4H), 1.36 (t, 12H, J = 6.5 Hz). The MS and ^{1}H NMR data are the same as those previously reported.[15]

Compound S11: TEA (78 µL, 0.55 mmol) was added to a mixture of Compound **S10** (106 mg, 0.19 mmol) and compound **S9** (70 mg, 0.19 mmol) in dried DMF (10 mL), and the reaction mixture was stirred under a nitrogen atmosphere overnight at room temperature. The solvent was removed under vacuum and the product was purified via silica gel column chromatography (eluent: dichloromethane/methanol/TEA, 250:5:1). Yield: 74%. MS (ESI): [M+Na]$^+$ calcd for $C_{48}H_{55}N_5O_6Na$, 820.42, found 819.84; ^{1}H NMR (500 MHz, CDCl$_3$): δ 7.91–7.86 (m, 5H), 7.49 (t, 2H, J = 8.8 Hz), 7.45–7.35 (m, 3H), 7.06 (dd, 1H, J = 5.5 Hz), 7.00 (d, 2H, J = 9.0 Hz), 6.43 (d, 2H, J = 8.5 Hz), 6.36 (d, 2H, J = 2.5 Hz), 6.25 (dd, 2H, J = 9.0 Hz), 4.17 (t, 2H, J = 4.8 Hz), 3.85 (t, 2H, J = 4.5 Hz), 3.68 (t, 2H, J = 4.5 Hz), 3.61 (t, 2H, J = 4.5 Hz), 3.51 (t, 2H, J = 4.8 Hz), 3.40 (t, 2H, J = 4.8 Hz), 3.40–3.30 (m, 10H), 3.18 (t, 2H, J = 7.3 Hz), 1.15 (t, 12H, J = 7.0 Hz); ^{13}C NMR (125 MHz, CDCl$_3$): δ 168.26, 161.33, 153.81, 153.25, 152.76, 148.74, 147.04, 132.39, 130.99, 130.38, 129.05, 128.86, 127.97, 124.72, 123.80, 122.74, 122.57, 114.85, 108.05, 105.50, 97.76, 70.83, 70.66, 70.49, 70.00, 69.57, 67.83, 67.71, 64.83, 44.37, 39.27, 12.63.

Compound S12: According to previous studies,[15-17] a side reaction, the cyclization of the amide into the center ring of the xanthene moiety to form spiro-isobenzofuran, occurred under the reaction conditions of Compound **S11** synthesis. The presence of the side product was confirmed by the new ^{13}C NMR signal at ~97.76 ppm,[16] which corresponds to the quaternary spiro carbon. Thus, compound **S11**

has no conjugated structure and no characteristic intense red color with the maximum absorbance at about 554 nm. The rhodamine B derivative fully regained the conjugation (**S12**) when trifluoroacetic acid was added to the solution.[17]

Prior to utilization in the study of rhodamine B-labeled azobenzene and surface PDMS-PEG-CD interactions, the *trans*- isomer of Compound **S12** was obtained by keeping its aqueous solution in the dark for one week; the presence of the *cis*-isomer was determined from the absorbance at 345 nm using an ultraviolet-visible (UV-Vis) spectrophotometer (Mapada UV-1600PC, China) in accordance with a previously reported method.[18]

Synthesis of FITC-labeled Azobenzene (Compound S13 in Scheme S5). Scheme S5 shows the synthesis of FITC-labeled azobenzene (Compound **S13** in Scheme S5). Compound **S9** (125 mg, 0.34 mmol, 1.3 equiv.) was dissolved in 3 mL dried DMF. Fluorescein-5-isothiocyanate (FITC, 100 mg, 0.26 mmol, 1.0 equiv) and TEA (54 μL, 0.39 mmol, 1.5 equiv) were then added to the reaction mixture. After stirring in the dark for 5 h, the solvent was removed under vacuum, and the product was purified through silica gel column chromatography (eluent: dichloromethane/methanol, 10:1). Yield: 21%. MS (ESI): $[M+Na]^+$ calcd for $C_{41}H_{38}N_4O_9SNa$ 785.2, found 785.7; ^1H NMR (500 MHz, CDCl$_3$): δ 9.10 (s, 1H), 7.90–7.70 (m, 6H), 7.50–7.30 (m, 5H), 7.10–6.90 (m, 4H), 6.70–6.40 (m, 5H), 4.09 (s, 1H), 3.90–3.40 (m, 15H).
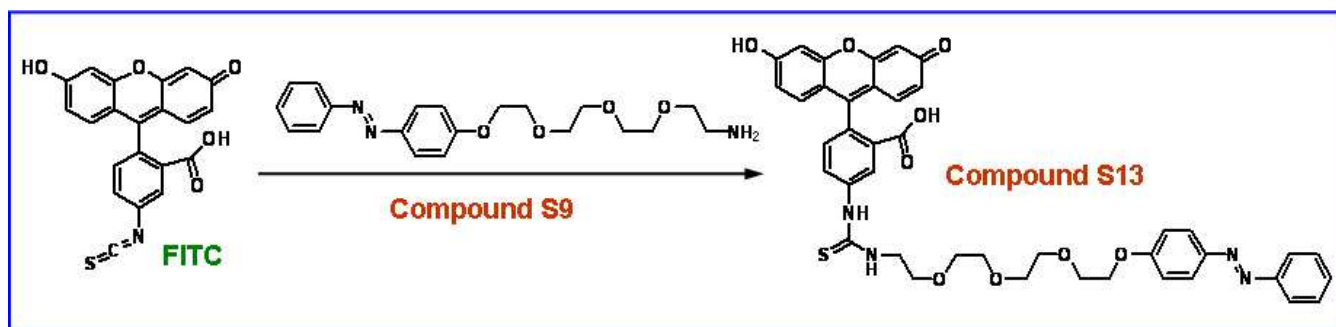
Scheme S5. Synthesis of FITC-labeled azobenzene (Compound **S13**).

Prior to utilization in the study of FITC-labeled azobenzene and surface PDMS-PEG-CD interactions, the *trans*-isomer of Compound **S13** was obtained by keeping its aqueous solution in the dark for one

week; the presence of the *cis*-isomer was determined from the absorbance at 345 nm using a UV-Vis spectrophotometer (Mapada UV-1600PC, China) in accordance with a previously reported method.[18]

AFM Investigation of the Native and Layer-by-layer Modified PDMS Surfaces. The surface morphology and the roughness of the native and modified PDMS surfaces were investigated through imaging using AFM technique. Figure S4 shows that the native PDMS surface was relatively flat with a roughness value of 1.58 nm for Rms and 1.25 nm for Ra. After silanization reaction, the roughness of the initiator-functionalized PDMS surface (PDMS-Br) increased to 2.08 nm for Rms and 1.71 nm for Ra, indicating that the surface PDMS-Br was successfully obtained. Also, the roughness of PDMS-PEG-Br surface increased to 7.00 nm (Rms) and 5.34 nm (Ra) after OEGMA6 was grafted onto the surface PDMS-Br. The formation of the nano-sized islands may result from the nano-scale phase aggregation of the grafted polymer chain after drying.[19] Compared with the surface PDMS-PEG-Br, there was no obvious surface morphology change (Rms = 7.27 nm, and Ra = 5.64 nm) for the surface PDMS-PEG-N$_3$ after azide groups were introduced on the surface PDMS-PEG-Br via nuceophilic substitution reaction. However, after coupling CD onto the PDMS-PEG-N$_3$ surface through click chemistry, the roughness of the surface PDMS-PEG-CD exhibited slight increase (7.42 nm for Rms, and 5.93 nm for Ra), which further verified that CD was successfully conjugated onto the PDMS surface by layer-by-layer modification.
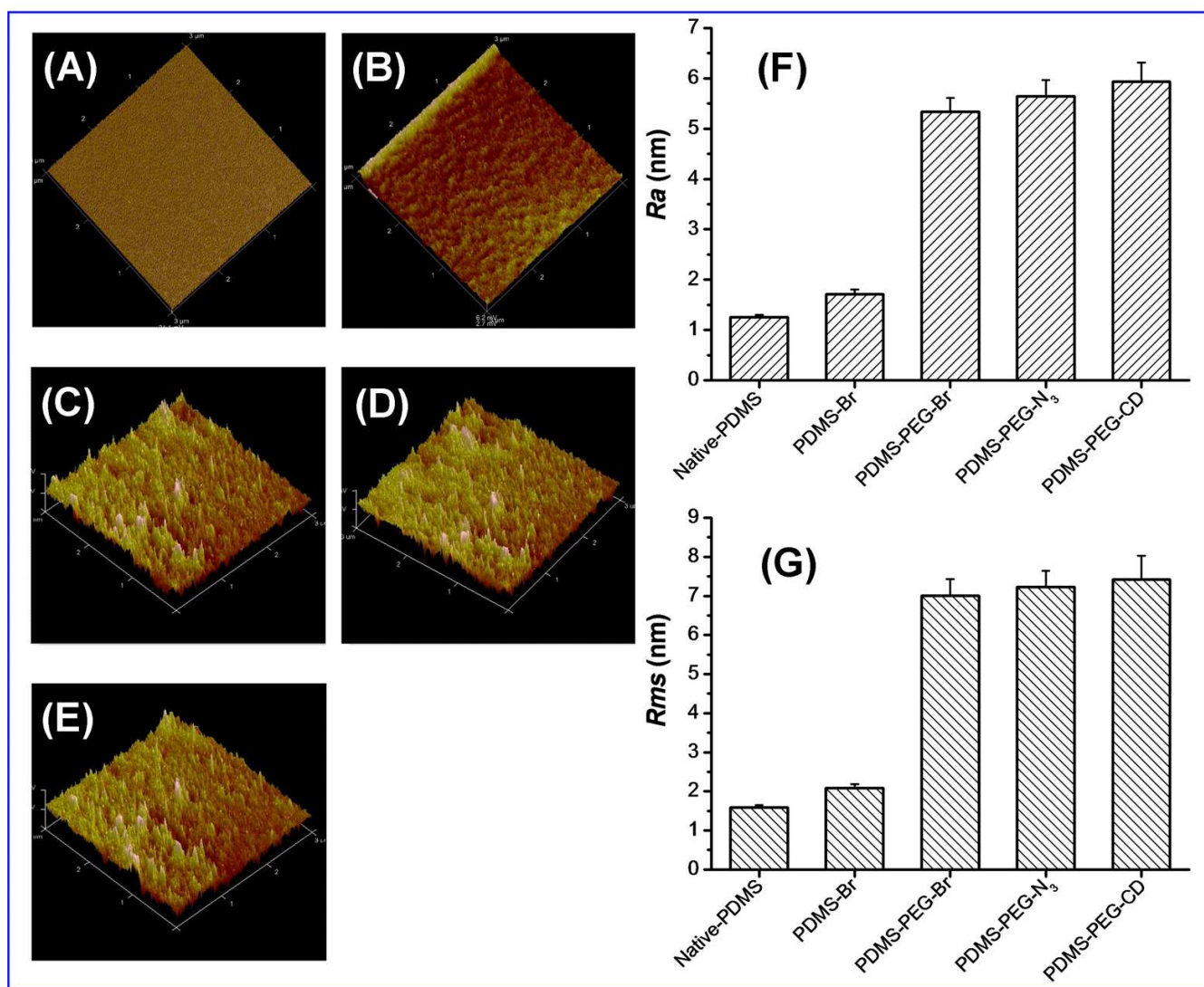
Figure S4. Tapping mode 3D images of one set of the native and layer-by-layer modified PDMS surfaces [(A) Native-PDMS; (B) PDMS-Br; (C) PDMS-PEG-Br; (D) PDMS-PEG-N$_3$; (E) PDMS-PEG-CD], and their corresponding roughness parameter Ra (F) and Rms (G) analysis [Native-PDMS, Ra = 1.25 ± 0.05 nm, Rms = 1.58 ± 0.06 nm (n=3); PDMS-Br, Ra = 1.71 ± 0.09 nm, Rms = 2.08 ± 0.10 nm (n=3); PDMS-PEG-Br, Ra = 5.34 ± 0.27 nm, Rms = 7.00 ± 0.42 nm (n=3); PDMS-PEG-N$_3$, Ra = 5.64 ± 0.32 nm, Rms = 7.27 ± 0.40 nm (n=3); PDMS-PEG-CD, Ra = 5.93 ± 0.38 nm, Rms = 7.42 ± 0.60 nm (n=3)].

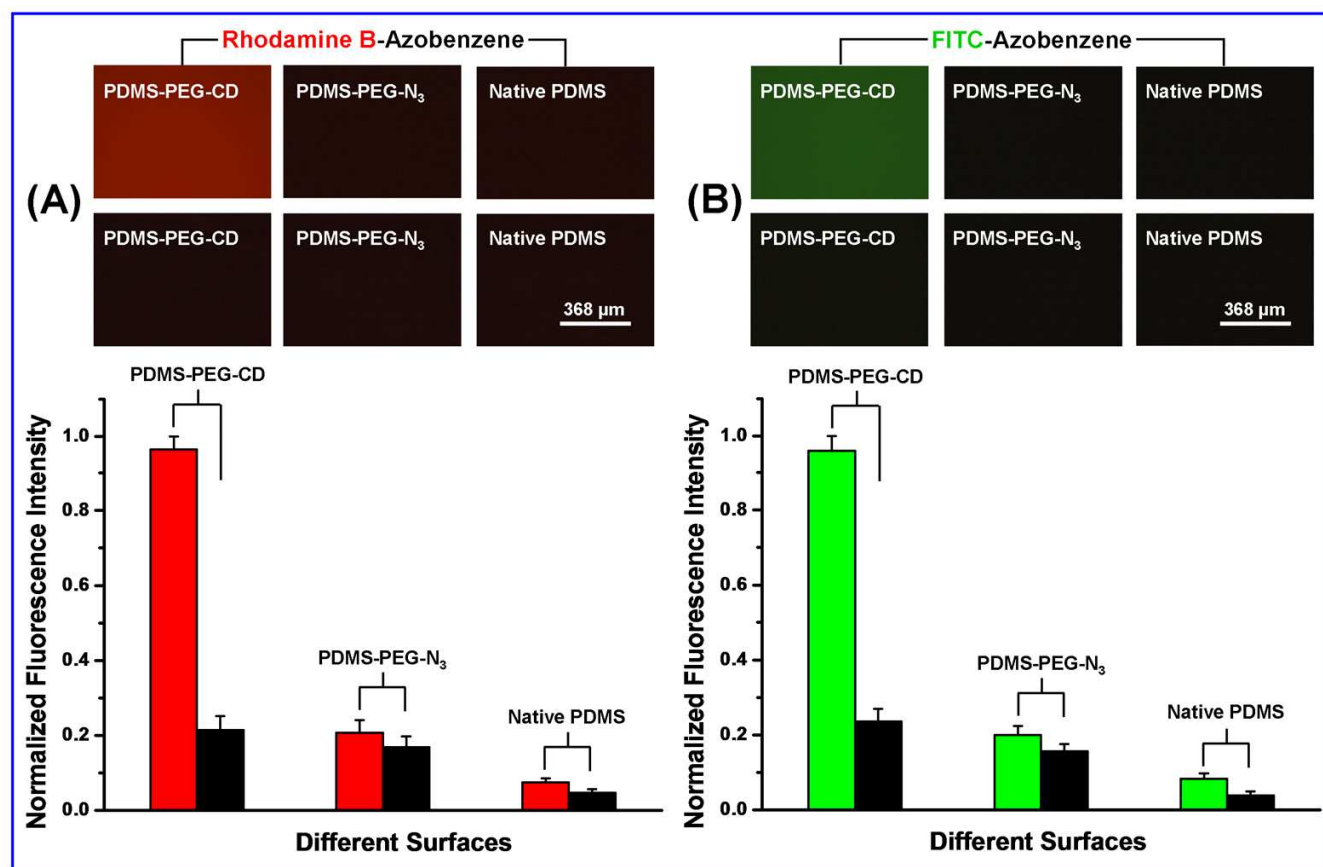**Reversible Interactions of Fluorophore-labeled Azobenzenes with Different PDMS Surfaces (Figure S5).**

Figure S5. Reversible interactions of fluorophore-labeled azobenzenes with PDMS-PEG-CD, PDMS-PEG-N$_3$, and native PDMS surface. (A) Rhodamine B-labeled azobenzene; (B) FITC-labeled azobenzene. The top two-line fluorescence images in (A) and (B) are the rhodamine B-labeled azobenzene- and FITC-labeled azobenzene-treated PDMS surfaces before (first line) and after UV irradiation (second line), respectively. The bottom histograms in (A) and (B) are the fluorescence intensity changes of rhodamine B-labeled azobenzene- (A) and FITC-labeled azobenzene- (B) treated PDMS surfaces before and after UV irradiation, respectively. Error bars represent ± SD (n = 3).
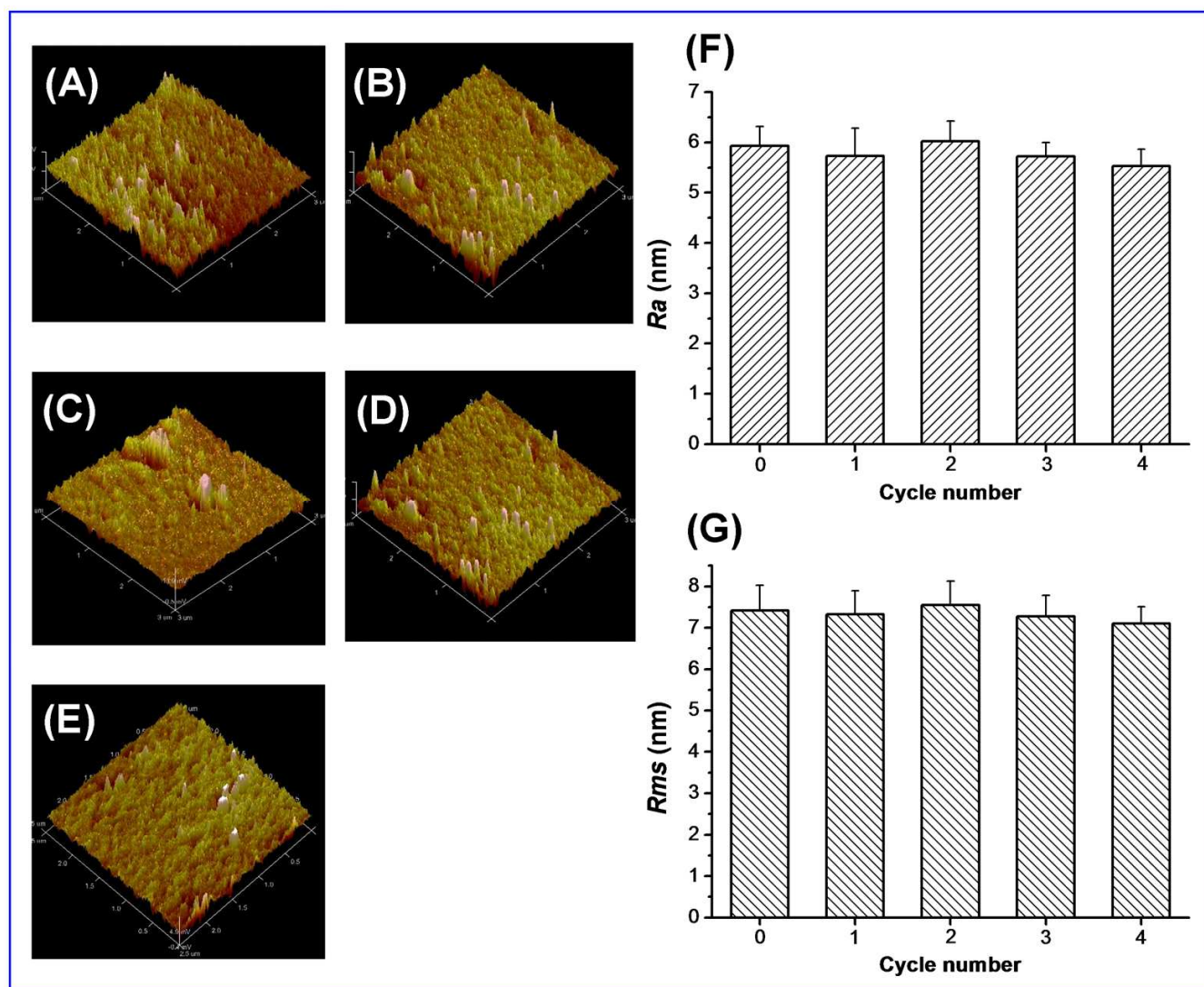
Figure S6. Tapping mode 3D images of one set of the PDMS-PEG-CD surfaces after each cycle in the study of photocontrolled reversible interactions between azobenzenes and PDMS-PEG-CD surfaces [(A) 0-cycle; (B) 1-cycle; (C) 2-cycle; (D) 3-cycle; (E) 4-cycle], and their corresponding roughness parameter Ra (F) and Rms (G) analysis [0-cycle, Ra = 5.93 ± 0.38 nm, Rms = 7.42 ± 0.61 nm (n=3); 1-cycle, Ra = 5.73 ± 0.55 nm, Rms = 7.33 ± 0.56 nm (n=3); 2-cycle, Ra = 6.02 ± 0.40 nm, Rms = 7.55 ± 0.57 nm (n=3); 3-cycle, Ra = 5.72 ± 0.27 nm, Rms = 7.27 ± 0.51 nm (n=3); 4-cycle, Ra = 5.53 ± 0.33 nm, Rms = 7.10 ± 0.41 nm (n=3)].
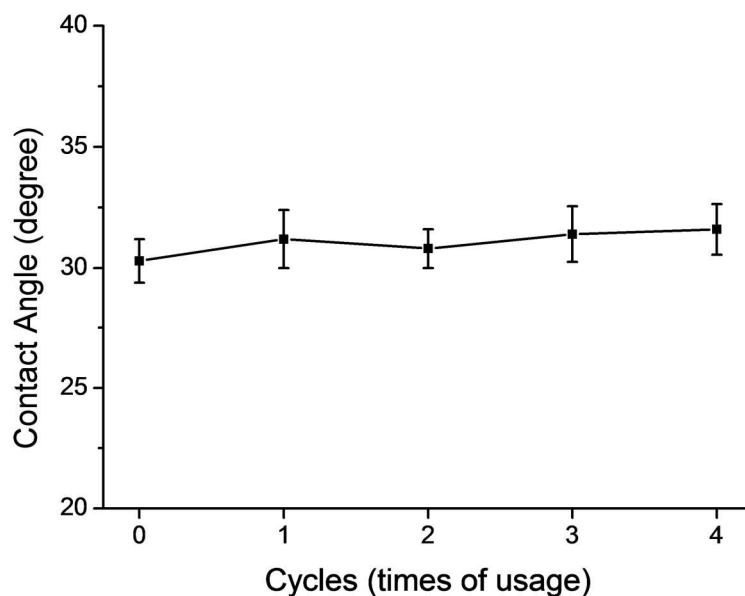
Figure S7. Contact angle measurement of the PDMS-PEG-CD surfaces after each cycle in the study of photocontrolled reversible interactions between azobenzenes and PDMS-PEG-CD surfaces.

Preparation of Azobenzene-grafted Primary Antibodies of Cardiac Biomarkers (Compound S15 in Scheme S6). Scheme S6 shows the preparation of azobenzene-grafted primary antibodies of cardiac biomarkers (Compound **S15** in Scheme S6), which consists of a two-step reaction.
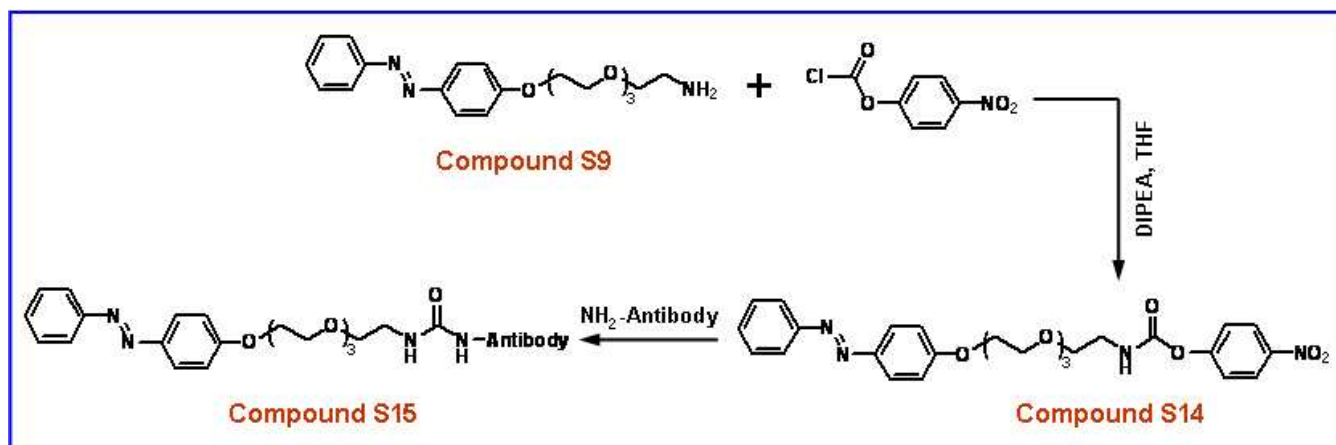
Scheme S6. Preparation of an azobenzene-grafted primary cardiac biomarker antibody (Compound **S15**) from amino-terminated azobenzene (Compound **S9**) and *p*-nitrophenyl carbonyl-terminated azobenzene (Compound **S14**) in the presence of the cardiac biomarker antibody anti-myoglobin 7C3 or anti-H-FABP 10E1.

Compound S14: Under a nitrogen atmosphere, *p*-nitrophenyl chloroformate (1 mmol, 0.2 g) and Compound **S9** (1 mmol, 0.37 g) were dissolved in 10 mL dried dichloromethane, N-ethyldiisopropylamine (1 mmol, 0.18 mL) was then added dropwise. The reaction mixture was stirred at room temperature for 6 h until the disappearance of Compound **S9**, which was confirmed via thin layer chromatography. The solution was washed with 1 mol/L hydrochloric acid three times. The organic phase was dried over anhydrous Na_2SO_4 and condensed. The residue was purified through silica gel column chromatography (eluent: dichloromethane/methanol, 3:1). Yield: 88%. MS (ESI): $[M+Na]^+$ calcd for $C_{27}H_{30}N_4O_8Na$, 561.21, found 561.11; ^1H NMR (500 MHz, $CDCl_3$): δ 8.22 (d, 2H, $J = 9.0$ Hz), 8.12 (d, 1H, $J = 9.0$ Hz), 7.90–7.85 (m, 3H), 7.52 (d, 2H, $J = 7.5$ Hz), 7.29 (d, 2H, $J = 9.0$ Hz), 7.02 (d, 2H, $J = 9.0$ Hz), 6.88 (d, 1H, $J = 9.0$ Hz), 6.12 (br, 1H), 4.23 (t, 2H, $J = 5.0$ Hz), 3.92 (t, 2H, $J = 5.0$ Hz), 3.80–3.50 (m, 10H), 3.49 (t, 2H, $J = 5.0$ Hz); ^{13}C NMR (125 MHz, $CDCl_3$): δ 162.45, 147.15, 144.76, 141.04, 130.54, 129.08, 126.11, 125.11, 124.71, 122.57, 122.07, 115.68, 114.77, 70.75, 70.58, 70.53, 70.17, 69.67, 69.63, 67.63, 41.19; IR: (ν, cm^{-1}) 3293.2, 2874.4, 1747.4, 1594.6, 1518.7, 1336.2, 1207.7, 1108.1, 839.9, 753.1, 689.2.

Azobenzene-grafted Antibody (Compound S15 in Scheme S6): The conjugation of Compound **S14** onto the desired antibody was performed following the previously reported methods,[20] with some modifications. Compound **S14** (5 µL, 24 mg/mL in DMF) was dissolved in 100 µL sodium phosphate buffer (pH 8.0), and the primary cardiac biomarker antibody (anti-myoglobin 7C3 or anti-H-FABP 10E1) solution [10 µL, 5.6 mg/mL in phosphate buffered saline (PBS, pH 7.4)] was added to the solution. The reaction was allowed to proceed for 3 h at 37 °C. The solution mixture was then extensively dialyzed against PBS (pH 7.4) with multiple buffer changes using a Slide-A-Lyzer mini-dialysis unit with a 3,500 Da molecular weight cut-off (Pierce Biotechnology, IL, USA) to remove excess Compound **S14.** The concentration was measured via the BCA protocol using a BCA Protein Assay Kit (Pierce Biotechnology, IL, USA).[21,22] Prior to use, the azobenzene‑grafted antibody solution was stored in a refrigerator at 4 °C.

Prior to utilization in the surface-based sandwich fluoroimmunoassay, the azobenzene‑grafted antibody solution was kept in the dark for one week to obtain the *trans-* isomer of Compound **S15**; the presence of the *cis*-isomer was determined from the absorbance at 345 nm using a UV-Vis spectrophotometer (Mapada UV-1600PC, China) in accordance with a previously reported method.[18]

Conventional Enzyme-linked Immunosorbent Assay (ELISA). To confirm the reliability of the PDMS-PEG-CD surface-based fluoroimmunoassay, a conventional ELISA was also performed in the current study for the determination of the cardiac markers myoglobin and H-FABP. The polystyrene wells of the ELISA strips (Nunc, Denmark) were coated with an anti-myoglobin 7C3 or anti-H-FABP 10E1 solution [10 μg/mL in 0.05 mol/L carbonate buffer (pH 9.6); 100 μL/well] overnight at 4 °C. They were subsequently treated with 1% BSA in PBS (150 μL/well) at 37 °C for 2 h to block nonspecific reactions. The serially diluted myoglobin or H-FABP samples were then placed in the primary cardiac marker antibody-coated wells (100 μL/well) and incubated at 37 °C for 1 h. Alkaline phosphatase-labeled anti-myoglobin 4E2 or alkaline phosphatase-labeled anti-H-FABP 9F3 was then added and the mixture was allowed to react at 37 °C for 1 h (the alkaline phosphatase-labeling kit-NH_2 was purchased from Dojindo, Tokyo, Japan, and the anti-myoglobin 4E2 and anti-H-FABP 9F3 labeling process was performed according to the manufacturer's instructions). After the addition of 100 μL/well *p*-nitrophenyl phosphate disodium salt (substrate of alkaline phosphatase; 1 mg/mL in diethanolamine buffer], the plates were incubated in the dark for 30 min at 37 °C (the alkaline phosphatase substrate kit, which consisted of *p*-nitrophenyl phosphate disodium salt and diethanolamine buffer, was from Thermo Scientific Inc., USA). Color development was stopped with 2 mol/L NaOH, and the absorbance was measured at 405 nm using a microplate reader (Bio-Rad model 680). The plates were washed three times with PBS (0.01 mol/L, pH 7.4) containing 0.05% Tween 20 between reaction steps. Each experiment was repeated at least three times. Blank controls were also run simultaneously during each experiment.

Figure S8 shows the relationship between the amount of biomarker detected (as revealed by the

absorbance values) and the actual biomarker concentration. The absorbance value increased when a higher concentration of analyte [cardiac marker myoglobin (A) or H-FABP (B)] was employed. The results are similar to those obtained from the PDMS-PEG-CD surface-based fluoroimmunoassay, in which the amount of biomarker detected was revealed by the fluorescence intensity (Figure 3 in the text).
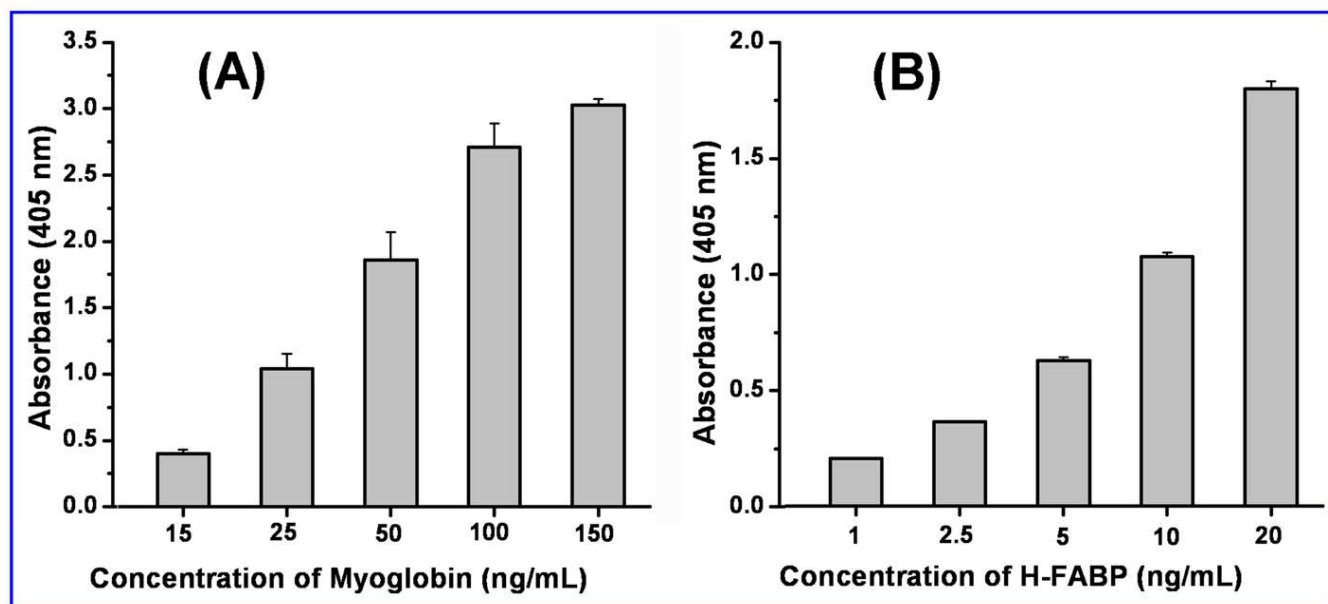

Figure S8. Relationship between the average absorbance at 405 nm obtained by ELISA and the cardiac marker concentration. (A) myoglobin, (B) H-FABP. Error bars represent ± SD (n = 3).

Specificity Assay. The specificity of antibodies for their antigens is very important for the sensitivity and accuracy of an assay. In the current study, the antibodies used were all commercialized monoclonal antibodies, which are intrinsically specific to their antigens. Control experiments for the specificity study of the current assay were also conducted. As shown in Figures S9(A) and S9(B), an increase in the fluorescence intensity was observed when the concentration of the target biomarker, myoglobin [Figure S9(A)] or H-FABP [Figure S9(B)] was increased, indicating that the azo-grafted primary antibody on surface PDMS-PEG-CD (anti-myoglobin 7C3 or anti-H-FABP 10E1 solution) showed obvious recognition of the target biomarker. However, the fluorescence intensity showed no obvious change with the increase in the concentration of the nontarget biomarker, which further confirms that the

interactions between the cardiac markers and their corresponding monoclonal antibodies immobilized on surface PDMS-PEG-CD are specific. The negligible response for H-FABP [Figure S9(A)] and for myoglobin [Figure S9(B)] is attributed to the combination of nonspecific surface adsorption and electrostatic interactions of the detection antibodies with the surfaces.
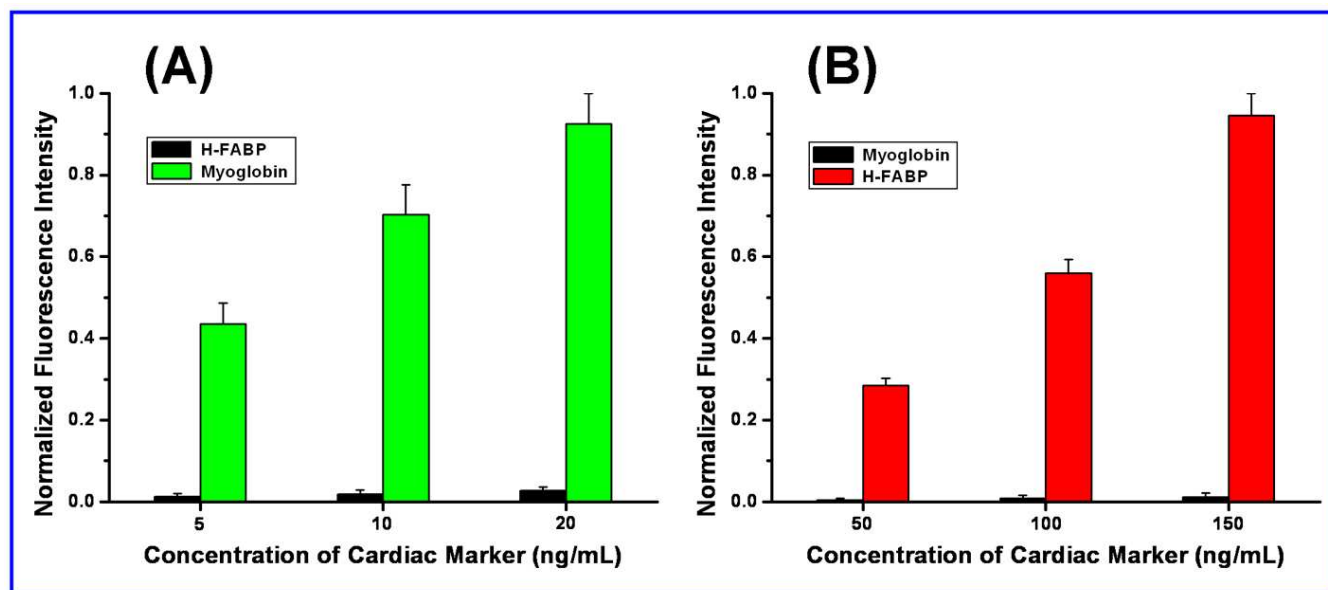

Figure S9. (A) Relationship between fluorescence intensity and myoglobin concentration. Control experiments were conducted using H-FABP. (B) Relationship between fluorescence intensity and H-FABP concentration. Control experiments were conducted using myoglobin. Error bars represent ± SD (n = 3).

REFERENCES

(1) Tugulu, S.; Arnold, A.; Sielaff, I.; Johnsson, K.; Klok, H. A. *Biomacromolecules* **2005**, *6*, 1602–1607.

(2) Diot, J.; García-Moreno, M. I.; Gouin, S. G.; Mellet, C. O.; Haupt, K.; Kovensky, J. *Org. Biomol. Chem.* **2009**, *7*, 357–363.

(3) Zhang, G. S.; Fang, L. Y.; Zhu, L. Z.; Sun, D. X.; Wang, P. G. *Bioorg. Med. Chem.* **2006**, *14*, 426–434.

(4) Brady, B.; Lynam, N.; O'Sullivan, T.; Ahern, C.; Darcy, R. *Org. Synth.* **2004**, *10*, 686–689.

(5) Casas-Solvas, J. M.; Martos-Maldonado, M. C.; Vargas-Berenguel, A. *Tetrahedron* **2008**, *64*, 10919–10923.

(6) Tokutake, S.; Oguma, T.; Tobe, K.; Kotani, K.; Saito, K.; Yamaji, N. *Carbohydr. Res.* **1993**, *238*, 193–213.

(7) Bonnet, V.; Duval, R.; Tran, V.; Rabiller, C. *Eur. J. Org. Chem.* **2003**, *19*, 4810–4818.

(8) Rana, S.; Lee, S. Y.; Cho, J. W. *Polym. Bull.* **2010**, *64*, 401–411.

(9) He, X. Y.; Yang, W.; Pei, X. W. *Macromolecules* **2008**, *41*, 4615–4621.

(10) Prucker, O.; Ruhe, J. *Langmuir* **1998**, *14*, 6893–6898.

(11) Marrani, A. G.; Dalchiele, E. A.; Zanoni, R.; Decker, F.; Cattaruzza, F.; Bonifazi, D.; Prato, M. *Electrochim. Acta* **2008**, *53*, 3903–3909.

(12) Zhao, Q.; Wang, S. F.; Cheng, X. J.; Yam, R. C. M.; Kong, D. L.; Li, R. K. Y. *Biomacromolecules* **2010**, *11*, 1364–1369.

(13) Wang, Z. H.; Wang, Y. M.; Luo, G. A. *Analyst* **2002**, *127*, 1353–1358.

(14) De, S.; Aswal, V. K.; Goyal, P. S.; Bhattacharya, S. *J. Phys. Chem. B* **1998**, *102*, 6152–6160.

(15) Srinivasan, B.; Huang, X. F. *Chirality* **2008**, *20*, 265–277.

(16) Anthoni, U.; Christophersen, C.; Nielsen, P.; Puschl, A.; Schaumburg, K. *Struct. Chem.* **1995**, *6*, 161–165.

(17) Miljanić, S.; Cimermana, Z.; Frkanec, L.; Žinić, M. *Anal. Chim. Acta* **2002**, *468*, 13–25.

(18) Auernheimer, J.; Dahmen, C.; Hersel, U.; Bausch, A.; Kessler, H. *J. Am. Chem. Soc.* **2005**, *127*, 16107–16110.

(19) Yu, W. H.; Kang, E. T.; Neoh, K. G. *J. Phys. Chem. B* **2003**, *107*, 10198–10205.

(20) David, C.; Hervé, F.; Sébille, B.; Canva, M.; Millot, M. C. *Sens. Actuators B* **2006**, *114*, 869–880.

(21) Wang, J.; Wang, X. Q.; Ren, L.; Wang, Q.; Li, L.; Liu, W.; Wan, Z.; Yang, L.; Sun, P.; Ren, L. L.; Li, M.; Wu, H.; Wang, J. F.; Zhang L. *Anal. Chem.* **2009**, *81*, 6210–6217.

(22) Wang, J.; Ren, L.; Wang, X. Q.; Wang, Q.; Wan, Z.; Li, L.; Liu, W.; Wang, X. M.; Li, M.; Tong, D.; Liu, A.; Shang, B. B. *Biosens. Bioelectron.* **2009**, *24*, 3097–3102.